



## Lyapunov–type numbers for Poincaré maps\*

K.D. Edoh and J. Lorenz

**ABSTRACT:** In [3] we have addressed computational issues related to Lyapunov–type numbers for invariant curves of planar maps. These numbers are important for understanding persistence and breakdown of the invariant curves when the map is perturbed. The purpose of this paper is to apply the results of [3] to Poincaré maps of systems of ODEs depending on a parameter and to address numerical issues involved.

**Key Words:** Invariant curves, arclength parametrization, invariant manifolds under perturbations, Lyapunov–type numbers.

### Contents

<b>1</b>	<b>Introduction</b>	<b>89</b>
<b>2</b>	<b>Lyapunov–Type Numbers</b>	<b>90</b>
2.1	The Case of a General Map . . . . .	90
2.2	The Case of a Poincaré Map . . . . .	92
<b>3</b>	<b>Numerical Results</b>	<b>93</b>
3.1	The Forced van der Pol Oscillator . . . . .	93

### 1. Introduction

Consider a first–order system of ODEs

$$\frac{dz}{dt} = f(z, \lambda, t), \quad z(t) \in \mathbb{R}^n, \quad (1.1)$$

depending on the real parameter  $\lambda$ . We assume that

$$f : \mathbb{R}^{n+2} \rightarrow \mathbb{R}^n$$

is a smooth map which is  $T$ –periodic in  $t$ , i.e,

$$f(z, \lambda, t + T) \equiv f(z, \lambda, t). \quad (1.2)$$

Let

$$z(t) = S(z_0, \lambda, t)$$

---

\* This work is partially supported by the FUTURES grant of North Carolina Agricultural and Technical State University, Greensboro USA.  
 2000 *Mathematics Subject Classification:* 65N35, 34C35, 58F27

denote the solution of (1.1) with  $z(0) = z_0$ . (We always assume the solution to exist for all  $t$  for the parameter values and initial data under consideration.) Then the map, from  $\mathbb{R}^n$  to  $\mathbb{R}^n$ , defined by

$$z_0 \rightarrow S(z_0, \lambda, T) =: P(z_0, \lambda)$$

is the Poincaré map corresponding to the  $T$ -periodicity of  $f$  for the fixed parameter value  $\lambda$ . If  $\Gamma(\lambda)$  is a simple closed curve in  $\mathbb{R}^n$  which is mapped bijectively onto itself by  $P(\cdot, \lambda)$ , then  $\Gamma(\lambda)$  is called invariant under  $P(\cdot, \lambda)$ . Upon identification of  $t = 0$  with  $t = T$ , the continuous-time dynamical system (1.1) has a corresponding invariant 2-torus,

$$\mathbb{T}(\lambda) \subset \mathbb{R}^n \times (\mathbb{R} \bmod T),$$

formed by the trajectories

$$\left( S(z_0, \lambda, t), t \right), \quad 0 \leq t \leq T, \quad z_0 \in \Gamma(\lambda).$$

An interesting and important question is under what assumptions an invariant torus  $\mathbb{T}(\lambda)$  gets merely deformed diffeomorphically as  $\lambda$  changes or gets destroyed (breaks) near certain  $\lambda$ -values. As explained in [1], generally one cannot assign a definite value of  $\lambda$  to the disappearance of an invariant torus, but the breakdown may be a chaotic process. (This may be unexpected from the point of view of standard bifurcation theory, based on Fredholm's alternative for linearized problems.) The linearized equations governing torus breakdown are not of Fredholm-type.)

However, *sufficient* conditions for the persistence of smooth invariant manifolds under small  $C^1$  perturbations of the governing vector field can be formulated in terms of so-called Lyapunov-type numbers. These numbers are determined by the linearized dynamics. For the general theory see, for example, [6].

In [3] we have specialized the general theory of Lyapunov-type numbers to the simple case of an invariant curve of a planar map and have addressed corresponding computational issues. The purpose of the present paper is to illustrate the results of [3], as well as numerical issues, in the case when the planar map is the Poincaré map of a continuous-time system (1.1) with  $n = 2$ . In Section 4, the periodically forced van der Pol oscillator is considered as a particular example. This is a much studied example for which invariant tori have been computed in [5], for example. As far as we know, the current paper is the first, however, which relates numerically computed Lyapunov-type numbers to the tori in the van der Pol oscillator. For a related case study, see [2].

## 2. Lyapunov-Type Numbers

We first define the Lyapunov-type numbers  $\nu(q)$ ,  $\bar{\nu}(q)$ ,  $\sigma(q)$ , and  $\bar{\sigma}(q)$  for the case where  $\Gamma$  is a simple closed  $C^1$  curve in  $\mathbb{R}^2$  which is invariant under an orientation preserving diffeomorphism  $P : \mathbb{R}^2 \rightarrow \mathbb{R}^2$ . For further details we refer to [3]. We then address numerical issues for the case where  $P$  is the Poincaré map of a dynamical system (1.1) with (1.2) and  $n = 2$ .

2.1. THE CASE OF A GENERAL MAP. Let  $P : \mathbb{R}^2 \rightarrow \mathbb{R}^2$  denote an orientation preserving diffeomorphism and let  $\Gamma \subset \mathbb{R}^2$  be a simple closed  $C^1$  curve which is mapped bijectively onto itself by  $P$ . For  $q \in \Gamma$  let  $T_q$  and  $N_q$  denote unit tangent and normal vectors to  $\Gamma$  in  $q$ , respectively. (Below, in (2.5), we assume that  $T_q$  and  $N_q$  are column vectors in  $\mathbb{R}^2$ .) We assume that the vectors  $T_q$  and  $N_q$  are oriented consistently along  $\Gamma$ , i.e, they depend continuously on  $q \in \Gamma$ . Let  $A_q = P'(q)$  denote the Jacobian of  $P$  at  $q$ . Invariance of  $\Gamma$  under the map  $P$  implies that

$$A_q T_q = a_q T_{P(q)}, \quad a_q > 0. \quad (2.3)$$

The number  $a_q$  measures local contraction (for  $0 < a_q < 1$ ) or expansion (for  $a_q > 1$ ) of the linearized dynamics *within*  $\Gamma$ . The vector  $A_q N_q$  can be decomposed as

$$A_q N_q = c_q T_{P(q)} + b_q N_{P(q)}, \quad b_q > 0. \quad (2.4)$$

The number  $b_q$  measures local contraction (for  $0 < b_q < 1$ ) or expansion (for  $b_q > 1$ ) of the linearized dynamics *towards*  $\Gamma$ . In matrix form, one obtains

$$A_q \begin{pmatrix} T_q & N_q \end{pmatrix} = \begin{pmatrix} T_{P(q)} & N_{P(q)} \end{pmatrix} \begin{pmatrix} a_q & c_q \\ 0 & b_q \end{pmatrix} \quad (2.5)$$

where the  $2 \times 2$  matrices  $\begin{pmatrix} T_q & N_q \end{pmatrix}$  and  $\begin{pmatrix} T_{P(q)} & N_{P(q)} \end{pmatrix}$  are orthogonal. This allows for an easy evaluation of  $a_q$  and  $b_q$  using (2.5).

To define  $\nu(q)$  we consider the sequence

$$\nu(q, n) = \left( b_q b_{P^{-1}(q)} \cdots b_{P^{-n}(q)} \right)^{1/(n+1)}$$

and set

$$\nu(q) = \limsup_{n \rightarrow \infty} \nu(q, n).$$

If  $\nu(q) < 1$  then let

$$\sigma(q, n) = \frac{\log \left( a_q a_{P^{-1}(q)} \cdots a_{P^{-n}(q)} \right)}{\log \left( b_q b_{P^{-1}(q)} \cdots b_{P^{-n}(q)} \right)} \quad (2.6)$$

and

$$\sigma(q) = \limsup_{n \rightarrow \infty} \sigma(q, n).$$

If  $\nu(q) < 1$  then  $\nu(q)$  measures the rate of attractivity towards  $\Gamma$ . Roughly, the smaller  $0 \leq \sup_q \nu(q) < 1$ , the stronger the attractivity of  $\Gamma$ . The number  $\sigma(q)$  measures the rate of the ratio<sup>1</sup> of attractivity within and towards  $\Gamma$ . If  $\nu(q) < 1$  and  $\sigma(q) < 1$  for all  $q \in \Gamma$ , then  $\Gamma$  can be shown to *persist* if a perturbation is added to  $P$  that is  $C^1$  small. Here persistence of  $\Gamma$  means that the perturbed map has an invariant curve close to  $\Gamma$ . If  $\sup_q \nu(q)$  approaches one during a continuation

<sup>1</sup> In general, this is finer than measuring the ratio of rates.

process, then  $\Gamma$  loses its attractivity. If  $\sup_q \sigma(q)$  approaches one, then the attractivity of the dynamics within  $\Gamma$  becomes as strong as the attractivity towards  $\Gamma$ , a situation which allows for the formation of non-smooth attractors replacing  $\Gamma$ . For a numerical case study, in which spiral points form on  $\Gamma$ , see [4].

The numbers  $\nu(q)$  and  $\sigma(q)$  measure the linearized dynamics in forward time, along a backward orbit that ends in  $q$ . One can also measure the linearized dynamics in forward time along a forward orbit that starts in  $q$ . This leads to the numbers  $\bar{\nu}(q)$  and  $\bar{\sigma}(q)$  defined as follows:

$$\bar{\nu}(q, n) = \left( b_q b_{P(q)} \cdots b_{P^n(q)} \right)^{1/(n+1)}, \quad \bar{\nu}(q) = \limsup_{n \rightarrow \infty} \bar{\nu}(q, n)$$

and, if  $\bar{\nu}(q) < 1$ ,

$$\bar{\sigma}(q, n) = \frac{\log \left( a_q a_{P(q)} \cdots a_{P^n(q)} \right)}{\log \left( b_q b_{P(q)} \cdots b_{P^n(q)} \right)}, \quad \bar{\sigma}(q) = \limsup_{n \rightarrow \infty} \bar{\sigma}(q, n).$$

**Remark:** Generally, the number  $\nu(q)$  differs from  $\bar{\nu}(q)$  and  $\sigma(q)$  differs from  $\bar{\sigma}(q)$ . Perturbation results for  $\Gamma$  can also be formulated in terms of  $\sup_q \bar{\nu}(q)$  and  $\sup_q \bar{\sigma}(q)$ . In [6], Fenichel considered *overflowing* invariant manifolds; for these, forward orbits  $q, P(q), \dots$  are generally not defined and the perturbation theory was worked out with  $\nu(q)$  and  $\sigma(q)$  instead of  $\bar{\nu}(q)$  and  $\bar{\sigma}(q)$ .

2.2. THE CASE OF A POINCARÉ MAP. In the following, we suppress the dependency on  $\lambda$  in our notation since it plays no role here. The evaluation of the Poincaré map  $P = P(q)$  requires the numerical solution of the initial-value problem

$$z_t = f(z, t), \quad z(0) = q,$$

for  $0 \leq t \leq T$ . One then has  $z(T) = P(q)$ . Correspondingly,  $P^{-1}(q) = z(0)$  if  $z(t)$  solves

$$z_t = f(z, t) \quad \text{for } 0 \leq t \leq T, \quad z(T) = q.$$

In the case  $n = 2$ , the accurate numerical evaluation of  $z(t)$  with high-order initial value codes typically causes no difficulty.

Let us address the evaluation of  $A_q = P'(q)$ , the Jacobian of  $P$  at  $q$ . We have considered two possibilities:

**a) Difference Approximation.** We have

$$(A_q)_{11} = \frac{\partial P_1}{\partial q_1}(q) \sim \frac{1}{2h} \left( P_1(q_1 + h, q_2) - P_1(q_1 - h, q_2) \right) \quad (2.7)$$

where  $h > 0$  is a step size. Similar expressions hold for  $(A_q)_{12}$  etc.

**b) Solution of an Initial-Value Problem.** Let  $z(t, q)$  denote the solution of

$$z_t = f(z, t), \quad z(0) = q, \quad (2.8)$$

and let  $D_q z(t, q)$  denote the Jacobian w.r.t.  $q$ . Differentiation of (2.8) w.r.t.  $q$  yields

$$D_q z_t = D_z f(z, t) D_q z, \quad D_q z(0) = I \quad (2.9)$$

where  $I$  is the  $2 \times 2$  identity matrix. Numerically, it is convenient to solve (2.8) and (2.9) together by treating the combined system as a system in 6 variables. Application of a high-order initial-value solver then yields

$$P(q) = z(T, q), \quad P'(q) = D_q z(T, q) .$$

We found that the numerical approach b) is generally preferable to a). It avoids the difficulty of choosing a good step size  $h$  in (2.7). Note that, if  $h$  is chosen too small, then the evaluations errors of  $P_1(q_1 \pm h, q_2)$ , which get divided by  $h$ , become dominant.

### 3. Numerical Results

We present three case studies for the periodically forced van der Pol oscillator. In Case 1 the Poincaré map has two fixed points on the invariant curve. This allows to determine the Lyapunov-type numbers in terms of eigenvalues and we have used it to validate the algorithm. Case 2 shows that, typically, the numbers  $\nu(q)$  etc. do not depend on  $q$ , but they depend, of course, on parameter values for the system. In Case 3 we relate the parameter dependence to bifurcations.

**3.1. THE FORCED VAN DER POL OSCILLATOR.** The van der Pol equation was originally introduced in the 1920s as a model for a simple vacuum tube oscillator circuit. In its periodically forced form it has become a much studied example of nonlinear dynamics.

We consider the equation in the form

$$\ddot{x} + \alpha(x^2 - 1)\dot{x} + x = \beta \cos(\omega t) \quad (3.10)$$

where  $\alpha, \beta$ , and  $\omega$  are real parameters. Under the transformations [7]

$$p(x) = x^3/3 - x, \quad y = \dot{x} + \alpha p(x), \quad (3.11)$$

the second-order equation (3.10) becomes the first-order system

$$\begin{aligned} \dot{x} &= y - \alpha p(x) \\ \dot{y} &= -x + \beta \cos(\omega t) . \end{aligned} \quad (3.12)$$

The system (3.12) takes the general form (1.1) with (1.2) and  $T = 2\pi/\omega$ .

Using the standard notations

$$\kappa = \beta/2\alpha \quad \text{and} \quad \rho = (1 - \omega^2)/\alpha$$

we present results for three cases:

**Case 1:** Let  $\alpha = \kappa = \rho = 0.4$ . The invariant curve  $\Gamma$  of the Poincaré map  $P$  is shown in Figure 1. In this case,  $P$  has two fixed points on  $\Gamma$ , namely

$$Q_1 = (2.086522, 0.992962) \quad \text{and} \quad Q_2 = (1.182570, -1.126298) .$$

Here  $Q_1$  is a sink, denoted by  $x$  in Figure 1, and  $Q_2$  is a saddle, denote by  $o$  in Figure 1. The eigenvalues of the Jacobian  $A_{Q_1}$  of  $P$  at  $Q_1$  are

$$\lambda_1 = 0.029751 \quad \text{and} \quad \lambda_2 = 0.788402 .$$

Here the eigenvector to the larger eigenvalue  $\lambda_2$  is tangential to  $\Gamma$ , and the smaller eigenvalue  $\lambda_1$  is the other eigenvalue of  $A_{Q_1}$ , measuring the rate of attractivity towards  $\Gamma$ . If  $q \in \Gamma$  is any point on the invariant curve  $\Gamma$  which is different from the saddle, then simple theoretical considerations (see [3]) show that one can express  $\bar{\nu}(q)$  and  $\bar{\sigma}(q)$  in terms of the eigenvalues of  $A_{Q_1}$  as follows:

$$\bar{\nu}(q) = \lambda_1 = 0.029751$$

and

$$\bar{\sigma}(q) = \frac{\log \lambda_2}{\log \lambda_1} = 0.067639 .$$

The eigenvalues of  $P$  at the saddle fixed point  $Q_2$  are

$$\lambda_1 = 0.324142 \quad \text{and} \quad \lambda_2 = 1.358307 .$$

Again, the eigenvector to the larger eigenvalue  $\lambda_2$  is tangential to  $\Gamma$  and the smaller eigenvalue  $\lambda_1$  is the other eigenvalue of  $A_{Q_2}$ , measuring the rate of attractivity towards  $\Gamma$ . Since  $\lambda_2 > 1$ , the fixed point  $Q_2$  is repelling in direction tangential to  $\Gamma$ .

If  $q$  is any point on  $\Gamma$  and  $q \neq Q_1$ , then backward orbits tend to  $Q_2$  and one obtains

$$\nu(q) = \lambda_1 = 0.324142$$

and

$$\sigma(q) = \frac{\log \lambda_2}{\log \lambda_1} = -0.271832 .$$

We have used these theoretically based results to test our algorithm, which approximates the numbers  $\nu(q)$ ,  $\bar{\nu}(q)$ ,  $\sigma(q)$  and  $\bar{\sigma}(q)$  using the formulae stated in Section 2.1. For the example described here, we obtained four digits of accuracy without difficulty.

**Case 2:** In this case,  $\alpha = 0.4$ ,  $\rho = 0.55$  and  $\beta$  varies in the interval  $0.38 \leq \beta \leq 0.3925$ . Invariant curves  $\Gamma = \Gamma(\beta)$  of the Poincaré map  $P = P(\cdot, \beta)$  are shown in Figure 2. These are in good agreement with the those of van Veldhuizen [8].

Numerical results for the Lyapunov-type number  $\nu = \nu(q, \beta)$  are shown in Figure 3. For fixed  $\beta$ , the variable  $q \in \Gamma$  is replaced by an angle variable,  $0 \leq \theta \leq 2\pi$ . The curves in Figure 3 are almost flat, showing that the dependency on  $q$  (or, equivalently, on  $\theta$ ) is very weak. On the other hand, the dependency on  $\beta$

is strong. When  $\beta$  increases beyond  $\sim 0.3925$  the invariant curve  $\Gamma(\beta)$  disappears in a sink. In terms of  $\nu(q, \beta)$ , this disappearance is connected with  $\nu$  approaching the value  $\nu = 1$ . We note that for the parameter values used in Figure 3 numerical computations show that  $\bar{\nu}(q, \beta) = \nu(q, \beta)$ . For the same parameter values we have also computed  $\sigma(q, \beta)$  and  $\bar{\sigma}(q, \beta)$ . These functions (not shown) turn out to be identically zero, saying that there is no attractivity of the linearized dynamics *within* the invariant curve  $\Gamma(\beta)$ .

**Case 3:** In Figures 5 and 6 we show the Lyapunov-type numbers  $\nu, \bar{\nu}, \sigma, \bar{\sigma}$  as functions of  $0.1 \leq \beta \leq 0.3418$  for  $\rho = \alpha = 0.4$ . (As in Case 2, there is practically no dependency on the point  $q \in \Gamma(\beta)$ .)

Previous numerical and analytical studies (see, for example, the bifurcation diagrams in [8,7,9]) have shown that for  $\beta$  less than  $\sim 0.275$  there is an attracting invariant curve  $\Gamma(\beta)$  and a source point  $S(\beta)$  in the region surrounded by  $\Gamma(\beta)$ . Representative curves  $\Gamma(\beta)$  are shown in Figure 4. A saddle point appears on  $\Gamma(\beta)$  at  $\beta \sim 0.275$  through a saddle-node bifurcation and splits into a sink and a saddle, located on  $\Gamma(\beta)$ , for larger values of  $\beta$ . In terms of the Lyapunov-type numbers, the saddle-node bifurcation at  $\beta \sim 0.275$  is clearly shown: For  $\beta > 0.275$  the values  $\nu(\beta)$  and  $\bar{\nu}(\beta)$  differ from each other, as do the values  $\sigma(\beta)$  and  $\bar{\sigma}(\beta)$ . This is expected since the appearance of a saddle and a sink on  $\Gamma(\beta)$  lead to different asymptotic behavior of the orbits that determine  $\nu$  and  $\bar{\nu}$  as well as  $\sigma$  and  $\bar{\sigma}$ .

As  $\beta$  approaches 0.3418, the saddle on  $\Gamma(\beta)$  collides with the source  $S(\beta)$  inside  $\Gamma(\beta)$ , leading to a second saddle-node bifurcation and the disappearance of  $\Gamma(\beta)$ . In terms of the Lyapunov-type numbers, this is indicated by  $\nu(\beta)$  approaching the value  $\nu = 1$ , i.e.,  $\Gamma(\beta)$  loses its attractivity.

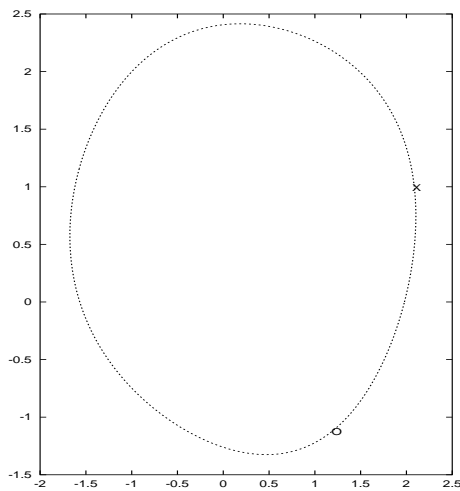


Figure 1: The invariant curve for the van der Pol oscillator with  $\alpha = \rho = 0.4$  and  $\beta = 0.32$ . The point  $x$  is a sink and  $o$  is a saddle.

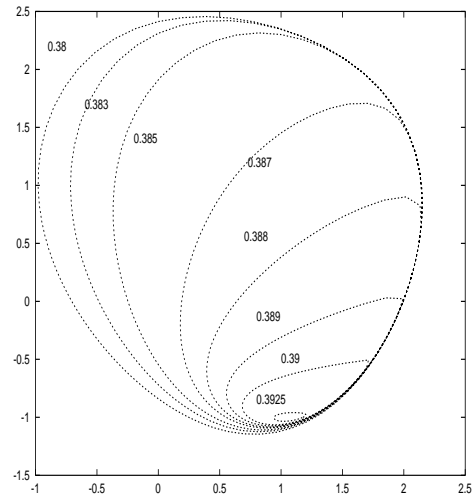


Figure 2: The invariant curves for van der Pol oscillator for  $\rho = 0.55$ ,  $\alpha = 0.4$  and  $0.38 \leq \beta \leq 0.3925$ .

## References

1. Aronson D. G., Chory M. A., Hall G. R., and McGehee R. P., *Bifurcation from an invariant circle for two parameter families of maps of the plane: a computer-assisted study*, *Comm. Math. Phys.*, 83, (1982), 303–354.
2. Dieci L., and Lorenz J., *Lyapunov-type numbers and torus breakdown: numerical aspects and a case study*, *Numerical Algorithms*, 14, (1997), 79–102.
3. Edoh K. D., and Lorenz J., *Computation of Lyapunov-type numbers for invariant curves of planar maps*, *SIAM J. Scientific Computing*, 23, No. 4, (2001), 1113–1134.
4. Edoh K. D., and Lorenz J., *Numerical approximation of rough invariant curves of planar maps*, *SIAM J. Scientific Computing*, 25, No. 1, (2003), 213–223.
5. Edoh K. D., Rusell R. D., and Sun W., *Computation of invariant tori by orthogonal collocation*, *Applied Numerical Analysis*, 32, (2000), 273–289.
6. Fenichel N., *Persistence and smoothness of invariant manifolds for flows*, *Indiana Univ. Math. J.*, 21, (1971), 193–226.
7. Guckenheimer J., and Holmes P., *Nonlinear Oscillations, Dynamical Systems and Bifurcation of Vector Fields*, Springer-Verlag, New York, 1983.
8. Van Veldhuizen M., *A new algorithm for the numerical approximation of an invariant curve*, *SIAM J. Sci. Stat. Comp.* 8, (1987), 951–962.
9. Reichelt V., *Computing invariant tori and circles in dynamical systems*, *IMA Vol. Math. Appl.* 119, Springer Verlag, New York, (2000), 407–437.



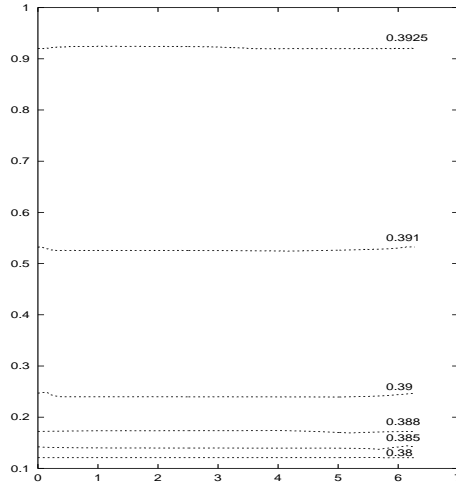


Figure 3: The values of  $\nu$  for the van der Pol oscillator with  $\rho = 0.55$   $\alpha = 0.4$ ,  $0.38 \leq \beta \leq 0.3925$  and  $0 \leq \theta \leq 2\pi$ .

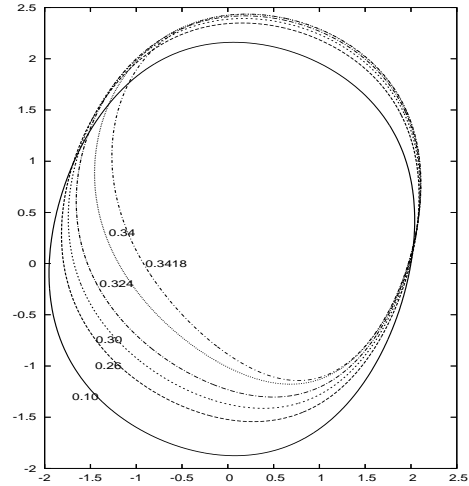


Figure 4: The invariant curves for the van der Pol oscillator with  $\rho = 0.55$   $\alpha = 0.4$  and  $0.1 \leq \beta \leq 0.3418$ .

*Kossi Edoh*  
 Department of Mathematics,  
 NC A&T State University  
 Greensboro, NC 27411 USA  
 kdedoh@ncat.edu

and

*Jens Lorenz*  
 Department of Mathematics and Statistics,  
 University of New Mexico  
 Albuquerque, NM 87131 USA  
 lorenz@math.unm.edu

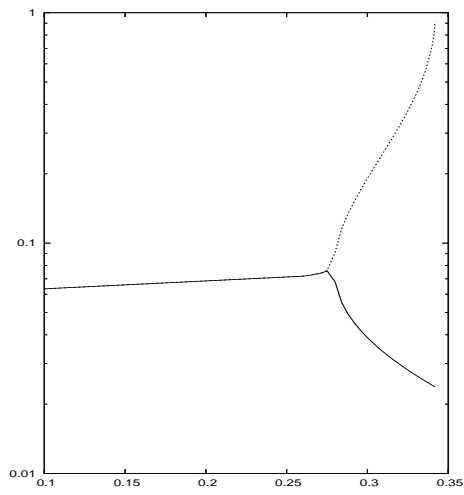


Figure 5: The values of  $\nu$  (dotted curve, up) and  $\bar{\nu}$  (solid line, down) for van der Pol oscillator with  $\alpha = \rho = 0.4$  and  $0.1 \leq \beta \leq 0.3418$ .

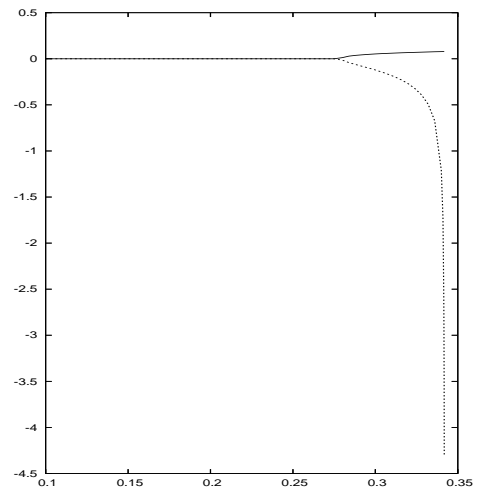


Figure 6: The values of  $\sigma$  (dotted curve, down) and  $\bar{\sigma}$  (solid curve, up) for van der Pol oscillator with  $\alpha = \rho = 0.4$  and  $0.1 \leq \beta \leq 0.3418$ .